pet tracers beyond [18F]FDG
A Technologists' Guide
www.eanm.org

EUROPEAN ASSOCIATION OF NUCLEAR MEDICINE

PET TRACERS BEYOND [18F]FDG

A TECHNOLOGISTS' GUIDE

Produced with the kind support of

SIEMENS Healthineers

[^{11}C]PE2I & [^{18}F]FE-PE2I

5

by Tea Crnic Bojkovic[1]
Jonathan Sigfridsson[1]
Vladimir Stepanov[2]
Jonas P. Eriksson[3]
My Jonasson[4]
Minyoung Oh[5]
Andrea Varrone[2]

[1] *Molecular Imaging and Medical Physics, Department of Surgical Sciences, Uppsala University, Uppsala, Sweden / Medical Imaging Centre, Uppsala University Hospital, Uppsala, Sweden*

[2] *Department of Clinical Neuroscience, Centre for Psychiatry Research, Karolinska Institutet and Stockholm Health Care Services, Stockholm, Sweden*

[3] *Department of Medicinal Chemistry, Uppsala University, 751 23 Uppsala, Sweden / PET Centre, Uppsala University Hospital, 751 85 Uppsala, Sweden*

[4] *Molecular Imaging and Medical Physics, Department of Surgical Sciences, Uppsala University, Uppsala, Sweden / Medical Physics, Uppsala University Hospital, Uppsala, Sweden*

[5] *Department of Clinical Neuroscience, Centre for Psychiatry Research, Karolinska Institutet and Stockholm Health Care Services, Stockholm, Sweden / Departments of Nuclear Medicine, Asan Medical Center, University of Ulsan College of Medicine, Seoul, Republic of Korea*

[11C]PE2I & [18F]FE-PE2I

Dopamine is the neurotransmitter that regulates motor functions, mood, and reward. Dopamine is released from axon terminals in the striatum or dendrites in the substantia nigra (SN). The action of dopamine on pre- and post-synaptic D1 and D2 dopamine receptors is terminated by the re-uptake of the neurotransmitter into presynaptic neuronal terminals through the dopamine transporter (DAT) (1). DAT density is higher in nigrostriatal axons and terminals but lower in the cell bodies and dendrites of the SN (2, 3).

[123I]FP-CIT (IOFLUPANE, DATSCAN) SPECT

is the most widely used modality for DAT imaging, authorised in Europe since 2000 and in the United States since 2011 (4, 5). DaTSCAN SPECT [123I] FP-CIT SPECT or DaTSCAN is indicated for the differential diagnosis of essential tremor from Parkinsonian syndromes related to idiopathic Parkinson's disease (PD), multiple system atrophy and progressive supranuclear palsy in patients with clinically uncertain Parkinsonian syndromes. It is also indicated to differentiate probable dementia with Lewy bodies from Alzheimer's dementia. Recently, PET imaging using [11C]PE2I and [18F]FE-PE2I has become a promising alternative offering high affinity and selectivity for DAT, favourable kinetics and improved spatial and temporal resolution (6, 7). This guide will provide an overview of the radiochemistry and in vivo properties of [11C]PE2I and [18F]FE-PE2I and how PET imaging with these radioligands is used in clinical practice.

CHEMISTRY & PROPERTIES

PE2I and FE-PE2I can both be viewed as structural derivatives of an earlier ligand, β-CIT, which has been extensively used for imaging DAT and SERT (serotonin transporters) (8). All three ligands share the same tropane backbone, commonly found in alkaloids contained in plants of the Erythroxylaceae and Solanaceae families. Many steps in the synthetic route for both PE2I and FE-PE2I are identical, as the compounds differ only in the alkyl chain on the tropane nitrogen. Much of the synthetic procedure is described in the original paper on PE2I synthesis by Emond and co-workers (9, 10), and it remains in use without significant changes. Given the complexities involved in building the tropane structure with the required stereochemistry from scratch, natural cocaine is used as a starting material for PE2I, FE-PE2I and their precursors due to its relative availability and low cost (Scheme 1).

PE2I(methyl-8-[(2E)-3-iodoprop-2-en-1-yl] -3-(4-methylphenyl)-8-azabicyclo[3.2.1] octane-2-carboxylate), along with the precursor for the synthesis of [11C]PE2I, desmethyl-PE2I (8-[(2E)-3-Iodoprop-2-en-1-yl]-3-(4-methylphenyl)-8-azabicyclo[3.2.1]

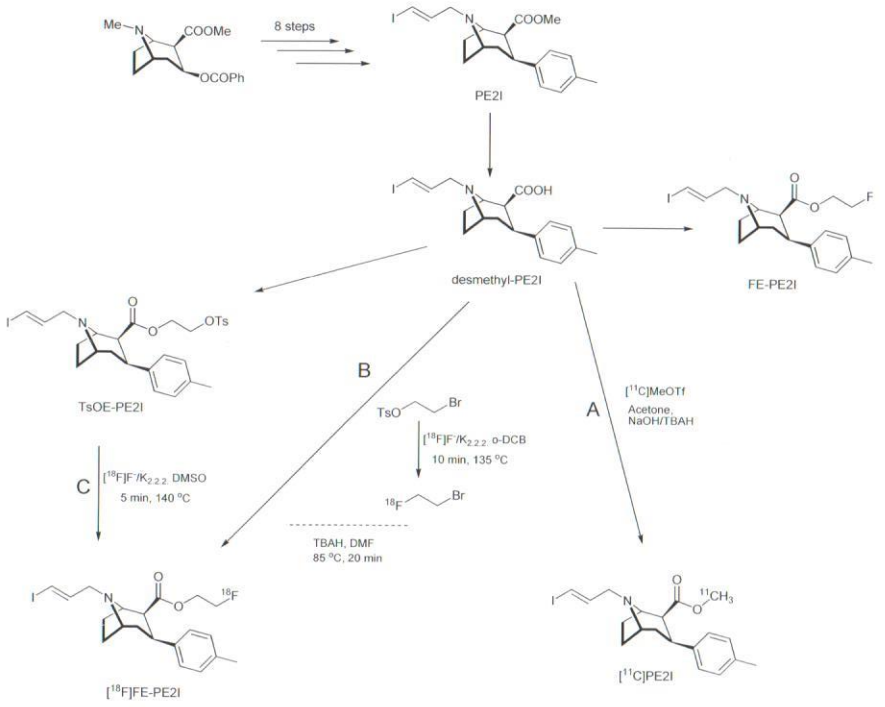

Scheme 1. Chemical structures of PE2I, FE-PE2I and synthesis of precursors. [11C]PE2I labelling (Pathway A). [18F]FE-PE2I 2-step labelling (Pathway B). [18F]FE-PE2I 1-step labelling (Pathway C).

octane-2-carboxylate), are solids with respective melting points of 75±5 °C and 167±5 °C. FE-PE2I (2-Fluoroethyl 8-[(2E)-3-iodoprop-2-en-1-yl]-3-(4-methylphenyl)-8-azabicyclo-[3.2.1]octane-2-carboxylate) and the precursor for [18F]FE-PE2I (tosylethyl-PE2I (2-(4-Methylphenylsulfonyl) ethyl 8-[(2E)-3-iodoprop-2-en-1-yl]-3-(4-methylphenyl)-8-azabicyclo-[3.2.1]octane-2-carboxylate)), are heavy-oil-like substances at room temperature that solidify at lower temperatures into a glassy material, a property that may complicate handling of small quantities. All four compounds are easily soluble in the majority of organic solvents; however, the tosylethyl-PE2I is unstable in aqueous solutions.

Radiosynthesis of [11C]PE2I

As with all carbon-11-labelled PET tracers, the radionuclide is produced by a cyclotron on-site. Carbon-11 is received as [11C]CO_2

or [^{11}C]CH_4 and the respective compound is then converted using the so-called wet method or the gas-phase method to [^{11}C] methyl iodide ([^{11}C]MeI), which in turn can be transformed into [^{11}C]methyl triflate ([^{11}C] MeOTf) for increased reactivity.

[^{11}C]PE2I can readily be synthesised from the O-desmethylated precursor, desmethyl-PE2I, using either [^{11}C]MeI or [^{11}C]MeOTf. The use of [^{11}C]MeOTf may be preferred due to the faster alkylation reaction and milder reaction conditions. The synthesis procedures were reported more than 20 years ago and are still widely used with minor modifications (11, 12) (Scheme 1, pathway A).

[^{11}C]PE2I is primarily synthesised using GBq quantities of [^{11}C]MeOTf transferred into a solution containing desmethyl-PE2I (0.4–0.6 mg) treated with a base (e.g., NaOH or TBAH) in acetone (300–600 µL). The reaction occurs nearly instantaneously at room temperature. In contrast, the use of [^{11}C]MeI typically requires heating to 80–90ºC and a reaction time of 5 minutes. The reaction mixture is then typically diluted, and obtained [^{11}C]PE2I is purified using HPLC (High Performance Liquid Chromatography), followed by reformulation and sterile filtration (11, 12) Since the early 2000s, when [^{11}C]PE2I was initially developed and reformulated by evaporation, reformulation methodologies have significantly advanced. More efficient solid phase extraction methods now dominate, offering high reliability and facilitating removal of residual polar impurities. These methods have largely replaced evaporation techniques. Similar approaches, or use of pharmaceutical HPLC-eluents that circumvents the reformulation step, have been applied to both [^{11}C]PE2I and [^{18}F]FE-PE2I (10, 13).

Radiosynthesis of [^{18}F]FE-PE2I

[^{18}F]FE-PE2I has been developed as a follow-up to [^{11}C]PE2I, partly because fluorine-18 offers several advantages for imaging and off-site preparation and distribution, and partly to overcome some unfavourable aspects of [^{11}C]PE2I kinetics (14, 15). The initial method, described by Schou and co-workers, is rather complex. It involves a reaction between desmethyl-PE2I and 2-bromo-1-[^{18}F]fluoroethane in dimethylformamide in the presence of sodium hydroxide (Scheme 1, pathway B) (14). The complexity of the original [^{18}F]FE-PE2I synthesis is largely attributed to the need for a simplified gas chromatography (GC) procedure for the purification of 2-bromo-1-[^{18}F]fluoroethane intermediate, making preparation of [^{18}F]FE-PE2I quite lengthy. However, development of a much simpler one-step labelling procedure (Scheme 1, pathway C) became possible with the introduction of a [^{18}F]FE-PE2I precursor suitable for direct labelling: tosylethyl-PE2I. This method was first published in 2012 by Stepanov et al. and was further refined by Bratteby and co-workers (13, 16).

Using the tosylethyl-PE2I precursor, [^{18}F]FE-PE2I can be obtained in a simple one-step, one-pot synthetic procedure performed in widely available solvents such as dimethylformaldehyde (DMF) and dimethyl sulfoxide (DMSO). This process involves trapping of the cyclotron-produced [^{18}F]fluoride on an anion-exchange cartridge, containing, for example, quaternary methylammonium resin (QMA), where it is concentrated and isolated from target water. The [^{18}F]fluoride is then typically eluted using a solution of $Kryprofix_{2.2.2}$/potassium carbonate in a water and acetonitrile mixture, followed by removal of the solvent in a drying step. Following the addition of the tosylethyl-PE2I precursor solution, the fluorination reaction proceeds within 5 min at elevated temperatures (e.g. 140 °C). The purification of [^{18}F]FE-PE2I is performed using HPLC, where a variety of approaches can be employed depending on the specifications of the synthetic module in use. It should be noted that [^{18}F]FE-PE2I is prone to radiolysis when trapped on SPE cartridges in large activity amounts (>1.5 GBq) or in aqueous solutions at high activity concentrations (>500 MBq/ml). Therefore, appropriate mitigation measures should be implemented, such as decreasing the activity concentration, increase of ethanol content, or addition of pharmaceutical-grade additives inhibiting radiolysis, such as sodium ascorbate and ascorbic acid.

QUALITY CONTROL PROCEDURES

Neither [^{11}C]PE2I nor [^{18}F]FE-PE2I are subjects of monographs in US or EU Pharmacopoeias. Therefore, in the absence of specifically described tests therein, general considerations for quality control apply (17). This includes a standard battery of quality control tests, such as tests for radiochemical purity, chemical purity, pH, filter integrity test, and residual solvents. Additionally, there are tests specifically for the [^{18}F]fluorine-labelled compounds, such as assessment of free [^{18}F]fluoride and Kryptofix content. Due to the short physical half-life of carbon-11 and fluorine-18, it is advised that lengthy quality control procedures should be conducted as post-release tests or on validation batches only (Table 1).

This is particularly relevant for radionuclide identification/radionuclidic purity tests and determination of endotoxins, and obviously a must for sterility tests on the formulated product. Other important control steps can only be carried out during the implementation of the production method. These can, for example, involve confirmation of the chemical structure using mass spectroscopy, ensuring high reproducibility of the synthesis, and ensuring that it yields sufficient activity amounts.

Comprehensive information on general procedures can, for example, be found in the general monograph on

Radiopharmaceutical Preparations (Ph. Eur 0125), in specific monographs written for other PET radiopharmaceuticals such as [18F]FDG and [11C]raclopride [Ph. Eur. 11.4, 1325 (01/2024); Ph. Eur. 11.4, 1924 (04/2023)] (18, 19), as well as in the scientific literature (13).

Quality control of [11C]PE2I

Due to the short half-life of carbon-11, pre-release testing is limited to the tests that are practically feasible to perform and mandatory for safe administration. Table 2 summarises the tests and analytical methods that can be used for quality control of [11C]PE2I.

Test	Pre-release	Post-release	Validation batches only
Radiochemical purity	X		
Product identification	X		
Radiochemical stability			X
Molar activity	X		
Filter integrity test	X		
Chemical purity	X		
pH	X		
Bacterial endotoxin test	X	X	
Residual solvents		X	
Sterility		X	
Radionuclidic purity			X
Confirmation of the carrier structure			X
Appearance			X
Residual Kryptofix	X		
Free [18F]fluoride	X		

Table 1. Pre-/post-release tests.

Test	Analytical method
Radiochemical purity	HPLC (with radiodetector)
Product identification	HPLC (with radiodetector)
Radiochemical stability	HPLC (with radiodetector)
Molar activity	With HPLC UV detector, scale and dose calibrator
Filter integrity test	as defined by Ph. Eur.
Chemical purity	HPLC (with UV detector)
pH	as defined by Ph. Eur.
Bacterial endotoxin test	as defined by Ph. Eur.
Residual solvents	GC
Sterility	as defined by Ph. Eur.
Radionuclidic purity	as defined by Ph. Eur.
Radionuclidic identity	as defined by Ph. Eur.
Appearance	as defined by Ph. Eur.

Table 2. Summary of tests and analytical methods for [11C]PE2I quality control.

Radiochemical purity of [11C]PE2I can be determined using Waters µ-Bondapak C18 10 µm, 3.9×300 mm column with acetonitrile/0.01 M H_3PO_4 35:65 as mobile phase at a flow rate of 3 ml/min with UV detector set to 254 nm. Chemical purity can be determined using ChromTech CP5-C18-25F 5 µm 4.6×250 mm column with acetonitrile/0.05M H_3PO_4 30:70 as mobile phase at flow rate 2 mL/min with UV detector set at 254 nm.

According to the European Pharmacopoeia monographs for other radiopharmaceuticals such as [18F]FDG and [11C]raclopride, the limit for bacterial endotoxins is 175 IU divided by the maximum recommended dose volume. Analysis can, for example, be performed using the Endosafe® nexgen-PTS™ system.

Quality control of [18F]FE-PE2I

A detailed description of Ph. Eur.-compliant Good Manufacturing Practice (GMP) quality control procedures can be found in (13) and Ph. Eur. 11.4, 1325 (01/2024) along with general considerations regarding quality control of radiopharmaceuticals described in (17). Table 3 summarises the tests and analytical methods that can be used for quality control of [18F]FE-PE2I.

Test	Analytical method
Radiochemical purity	HPLC (with radiodetector)
Product identification	HPLC (with radiodetector)
Radiochemical stability	HPLC (with radiodetector)
Molar activity	With HPLC UV detector, scale and dose calibrator
Filter integrity test	as defined by Ph. Eur.
Chemical purity	HPLC (with UV detector)
pH	as defined by Ph. Eur.
Bacterial endotoxin test	as defined by Ph. Eur.
Residual solvents	GC
Sterility	as defined by Ph. Eur.
Radionuclidic purity	as defined by Ph. Eur.
Radionuclidic identity	as defined by Ph. Eur.
Appearance	as defined by Ph. Eur.
Residual Kryptofix	as defined by Ph. Eur.
Free [18F]fluoride	as defined by Ph. Eur.

Table 3. Summary of tests and analytical methods for [18F]FE-PE2I quality control.

Radiochemical purity of [18F]FE-PE2I can be determined using Waters µ-Bondapak C18 10 µm, 3.9×300 mm column with acetonitrile/0.01 M H_3PO_4 35:65 as mobile phase at a flow rate of 2.5 ml/min with UV detector set to 254 nm. Chemical purity can be determined using Waters µ-Bondapak C18 10µm, 3.9×300 mm column with acetonitrile/0.01M H_3PO_4 30:70 as mobile phase at a flow rate of 2.5 ml/min with UV detector set to 254 nm. Alternative reverse-phase chromatography methods can be successfully employed as well (13, 16). Use of basic eluents for quality control of [18F]FE-PE2I can be beneficial, as it allows for LC determination of free [18F]fluoride (16, 20).

Residual Kryptofix is determined using a spot colorimetric threshold test as defined by Ph. Eur. The presence of sodium ascorbate, if added for improved stability of [18F]FE-PE2I in the formulation, can interfere with standard colorimetric tests, therefore it is imperative to perform a specificity test to confirm that Kryptofix can be successfully determined in the formulation used. Other quality control tests are performed to the standards defined in Ph. Eur. for [18F]FDG, where applicable [Ph. Eur. 11.4, 1325 (01/2024)] (19).

PHYSIOLOGICAL BIODISTRIBUTION

[11C]PE2I and [18F]FE-PE2I exhibit high affinity and remarkable selectivity for dopamine transporters (DAT) over serotonin and noradrenaline transporters (7).

[11C]PE2I

Several [11C]PE2I studies evaluated the whole-body biodistribution, radiation-absorbed doses and DAT quantification with PET in-vivo in humans (21-23). These studies have shown that ten minutes after administration of [11C]PE2I, the highest radioactivity concentration is observed in the kidneys, intestines, liver, stomach, salivary glands, vertebral bodies and the brain. Subsequently, 55–112 min after injection, most of the radioactivity accumulates in the urinary bladder.

[11C]PE2I undergoes rapid metabolism with predominant renal clearance and achieves peak blood–brain barrier penetration at 10 min post-injection. The highest uptake in the brain is observed in the striatum, where the concentration, in physiological conditions, remains constant from 10–60 min post-injection and decreases slowly between 1 and 2 h post-injection. The uptake of [11C]PE2I in the midbrain — SN — is lower than in the striatum. The thalamus shows some [11C]PE2I uptake, whereas the uptake in the cerebellum and other cortical regions is very low.

[18F]FE-PE2I

After intravenous administration of [18F]FE-PE2I, the highest activity concentration is observed in the liver between 10 and 30 min after injection, and in the gallbladder at 1 to 6 h after injection. At 6 h after injection, the gallbladder, the small intestine, the salivary glands, and the red marrow showed the highest activity concentration (24).

[18F]FE-PE2I rapidly enters the brain, with highest uptake in the striatum at approximately 10 min post-injection, and has a rapid washout of between 20 and 90 min post-injection. The metabolism of [18F]FE-PE2I is relatively fast. At 20 min, the unchanged radioligand in plasma is 20–25% of the total radioactivity, decreasing to 10–15% at 60 min after injection (24). [18F]FE-PE2I provides faster washout from the brain than [11C]PE2I and lower production of a radiometabolite that crosses the blood-brain barrier (25).

Overall, these properties permit the visualisation and quantification of DAT in the entire nigro-striatal system, which has been challenging due to the small size and low DAT density of the SN (26). The binding is predominantly distributed in the bilateral caudate nucleus and putamen, followed by the SN, with symmetrical and even distribution (27). Figure 1 shows the distribution of [11C]PE2I and [18F]FE-PE2I in the brain at different time points after injection in a healthy subject, together with time-activity curves in striatum

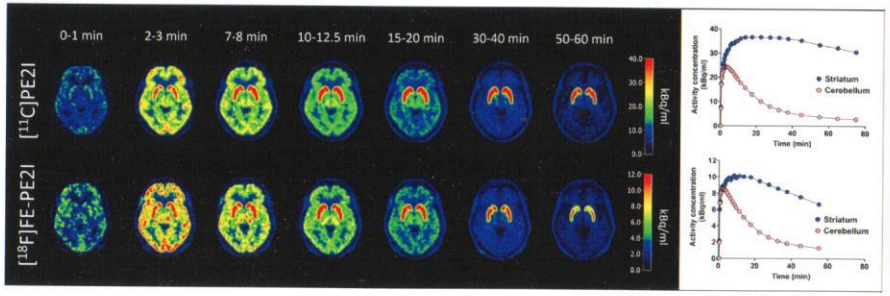

Figure 1. Distribution of [11C]PE2I (top row) and [18F]FE-PE2I (bottom row) in one healthy subject at different time points and time-activity curves in striatum (high-density region) and cerebellum (reference region).

(high-density region) and cerebellum (reference region).

PATIENT PREPARATION & AFTERCARE

Patient preparation for both [11C]PE2I and [18F]FE-PE2I is similar to the preparation before DAT SPECT examinations with [123I]β-CIT or [123I]FP-CIT. While the SPECT tracers also bind to the serotonin and noradrenaline transporters to some extent, the PE2I compounds are very selective for DAT. This means that medications that affect serotonin and noradrenaline re-uptake affect the DAT SPECT investigation, but they affect PE2I PET to a (much) lesser extent.

Before patient arrival, it is important to collect information about medications or drugs that bind competitively to DAT and could thus cause false positive results. Several drugs of abuse, mainly cocaine and amphetamine, have strong affinity for DAT and should be completely avoided before PE2I imaging. It is advised to refer to the EANM guideline/SNMMI procedure standard (27) for the list of drugs binding to the DAT that might interfere with the PET examinations. While discontinuation of medications targeting DAT should be considered, it is important to consider the risk to the patient, and such decisions should therefore be taken on an individual basis. In several cases, the risk outweighs the benefit of discontinuing medications before the examination.

Dynamic imaging with [11C]PE2I and [18F]FE-PE2I enables the measurement of relative cerebral blood flow (rCBF) and DAT availability in the same imaging session (see section on Quantification). If rCBF is measured, efforts should be made to reduce intake of food and common stimulants that affect the haemodynamics in the brain. Fasting for two to four hours before radiopharmaceutical injection is recommended and generally well tolerated. Caffeine, in its role as an adenosine receptor antagonist, can lower CBF and should be avoided before examination. Nicotine and alcohol are other blood flow-altering substances which should be avoided prior to a PE2I examination.

The patient should be positioned comfortably in the PET system using a head support and a support for the arms. Extra effort should be taken to secure the head position to reduce the risk of involuntary motion that might hamper image quality. The patient's brain should be positioned in the isocentre of the scanner. This is particularly important if a diagnostic CT scan is performed during the examination. When performing a dynamic scan to measure relative rCBF, it is preferable to dim the lights in the room and avoid loud noises during the early phase of the acquisition in order to reduce the impact on blood flow in the visual and auditory cortex, respectively.

IMAGING PROTOCOL (EQUIPMENT, IMAGING PARAMETERS)

[11C]PE2I and [18F]FE-PE2I PET can be performed using either dynamic or static acquisition. The most common protocol used in routine practice is static acquisition, since it is more clinically feasible, allows for higher patient throughput, and requires less post-processing. A static acquisition at 30–40 min p.i. is recommended for routine clinical use of both tracers (27).

Image reconstruction

Image reconstruction, whether for a dynamic or static scan, should be performed according to vendor recommendations. Reconstructions should, if possible, include time-of-flight (TOF) and point spread function (PSF) modelling. However, it is important that all patients in a given centre are evaluated using the same reconstruction parameters. To provide a reliable assessment when the interpretation is aided by comparison to a normal database, the reconstruction of PET data acquired in the patient should be equivalent to the reconstruction used for the PET data acquired in the subjects in the normal database. When performing dynamic acquisitions, shorter frame lengths of ≤60 s are used at the beginning of the acquisition, while 5–10-min frames are sufficient during the later phase. Short frame length in the early phase is especially relevant for the calculation of rCBF.

Quantification

Dynamic imaging allows for absolute quantification of DAT availability. The simplified reference tissue model (SRTM), using grey matter in the cerebellum or occipital cortex as the reference region, can provide the non-displaceable binding potential (BP_{ND}) without the need for

arterial sampling. BP_{ND} is directly proportional to the concentration of available dopamine transporters. From the same acquisition, it is also possible to calculate relative tracer delivery (R_1), providing an estimate of rCBF. Assessment of rCBF can aid in differentiation between idiopathic Parkinson's disease and atypical Parkinsonian syndromes (28).

Dynamic imaging for measurement of BP_{ND} using SRTM requires at least 80 min for [11C]PE2I (29), whereas an acquisition time of 60 min is sufficient for [18F]FE-PE2I due to its faster in vivo kinetics (25). Simplified measures can be estimated using shorter scan durations. Using a static acquisition at around 30–40 min p.i., it is possible to calculate the specific binding ratio (SBR) between striatum and a reference region (28, 30, 31). This is calculated as the ratio of the activity concentration in striatum minus the activity concentration in the reference region divided by the activity concentration in the reference region and equals the standardised uptake value ratio minus one. SBR corresponds well with BP_{ND} and allows for discrimination of patients with and without Parkinson's disease (30, 32). A 0–40 min dynamic acquisition can, in addition to SBR, also yield rCBF measurements for dual parameter investigation (32). Using a basis function implementation of SRTM, both BP_{ND} and rCBF can be estimated at the voxel level, allowing for visualisation of DAT availability and rCBF as parametric images (29). The hemisphere asymmetry index calculated as (Right-Left)/(Right+Left) or the putamen-to-caudate ratio can be useful in borderline cases (27).

RESULTS & INTERPRETATION (TYPICAL ABNORMAL FINDINGS / UPTAKE AND EXAMPLES)

An advantage of dynamic PET acquisitions lies in the ability to perform pharmacokinetic analyses, thus obtaining quantitative parameters. For both [11C]PE2I and [18F]FE-PE2I, BP_{ND} or SBR to measure DAT availability, as well as rCBF, corresponding to overall brain function, can be calculated and visualised as parametric images (28).

A comparative analysis investigated the use of dynamic [11C]PE2I PET as a stand-alone method versus the dual-modality approach using [123I]FP-CIT SPECT and 2-[18F]FDG PET (28). Strong consistency between [11C]PE2I BP_{ND} and [123I]FP-CIT SPECT images was observed, showing superior image quality for [11C]PE2I BP_{ND}. Moreover, there was a strong correlation between rCBF and 2-[18F]FDG PET images. The relationship between rCBF and 2-[18F]FDG across the regions was slightly inhomogeneous, with somewhat higher correlations in cortical regions than in subcortical regions, but with similar disease patterns overall. This implies that the disease patterns for [123I]FP-CIT SPECT and 2-[18F]FDG PET described in recent EANM guidelines are applicable to dynamic [11C]PE2I PET in differential diagnosis of Parkinsonian disorders (27, 33).

Integration with structural imaging (CT, MRI) expands the diagnostic potential, providing a comprehensive one-stop solution for patients with Parkinsonian disorders. In a recent study, a within-subject comparison of [11C]PE2I and [18F]FE-PE2I was performed, showing a high correlation regarding both measures of DAT availability and rCBF (34).

Evaluation of PE2I PET images involves careful visual examination in the axial, sagittal and coronal planes, and the interpretation should also take account of anatomical information from structural imaging (CT, MR). Visual interpretation can be supported by semi-quantification methods, such as the three-dimensional stereotactic surface projections (3D SP) method developed for [18F]FDG (35, 36). To enhance visual analysis, a 3D SP perfusion map can be generated through voxel-based analysis of rCBF, by normalising activities against a reference region and comparing them to a normal control database. Reference to the 3D-SSP images (Figure 3 and 4).

Ideally, the reference region should be unaffected by the disease and cerebellum is used in most cases. Alternatively, the occipital cortex may be used. A simplified

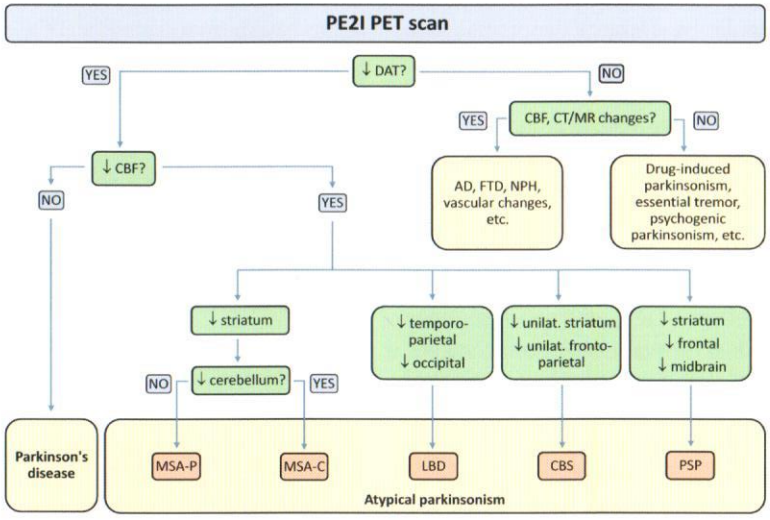

Figure 2. A simplified diagnostic algorithm chart for dynamic [11C]PE2I PET and [18F]PE2I PET scans. Image adopted from recent EANM guidelines (2, 3). DAT, dopamine active transporter; CBF, cerebral blood flow; AD, Alzheimer's disease; FTD, frontotemporal dementia; NPH, normal pressure hydrocephalus; MSA-P, multiple system atrophy-Parkinsonian type; MSA-C, multiple system atrophy-cerebellar type; LBD, dementia with Lewy bodies; CBS, corticobasal syndrome; PSP, progressive supranuclear palsy.

diagnostic algorithm chart for dynamic [11C]PE2I PET and [18F]PE2I PET scans is presented in Figure 2.

In general, DAT ligand binding is observed in Parkinson's disease and atypical Parkinsonian syndromes. However, differentiation at this level is challenging due to the significant overlap between disease patterns. To distinguish Parkinson's disease from different types of atypical Parkinsonian syndrome, the evaluation of rCBF images is essential for detecting typical topographic patterns of blood flow alterations. Furthermore, structural imaging helps evaluate other types of changes that could be causing symptoms, such as vascular changes or normal pressure hydrocephalus. Figures 3 and 4 depict typical abnormal findings in a patient with Parkinson's disease and progressive supranuclear palsy, respectively.

Longitudinal DAT changes measured with [18F]FE-PE2I or [11C]PE2I PET

Age-related DAT decline has been reported in several single-centre studies; however, the largest pool of normative data has been generated by two large multicentre studies performed in healthy subjects. The first is the ENC-DAT (European Normal Control Database of DaTSCAN) database, which includes [123I]FP-CIT SPECT data acquired in 13 different centres from 139 healthy controls (74 men, 65 women) with an age range between 20 and 83 years (37). The second database was acquired as part of the Parkinson's Progression Marker Initiative (PPMI) and includes [123I]FP-CIT SPECT data of 196 healthy controls examined longitudinally over 3 to 4 years (38). The age-related DAT decline reported by these two multicentre studies was 5.5–6% per decade (0.6%/year).

In Parkinson's disease, the average annualised DAT decline measured with [18F]FE-PE2I was 5% to 8.5% for the caudate, putamen and sensorimotor striatum, whereas negligible DAT changes have been reported for the substantia nigra (31, 39). Figure 5 shows [18F]FE-PE2I BP_{ND} images in a PD patient with longitudinal follow-up and an age-matched healthy control. Similar results have been reported for [11C]PE2I PET.

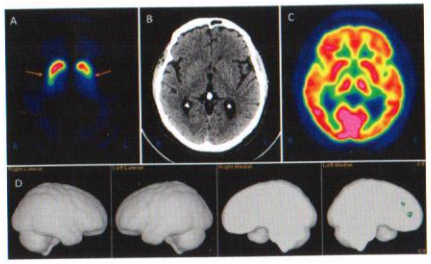

Figure 3. Example of [11C]PE2I PET/CT images in a patient with Parkinson's disease with predominantly right-sided clinical symptoms. (A) [11C]PE2I images of DAT availability showing asymmetrically reduced uptake in striatum (orange arrows), more pronounced on the left side. (B) CT image at the level of striatum showing no abnormalities. (C) [11C]PE2I image of rCBF showing normal perfusion in the cortex and striatum. (D) 3D surface projection map showing perfusion z-scores compared to a healthy control database, indicating perfusion in the normal range in all cortical regions.

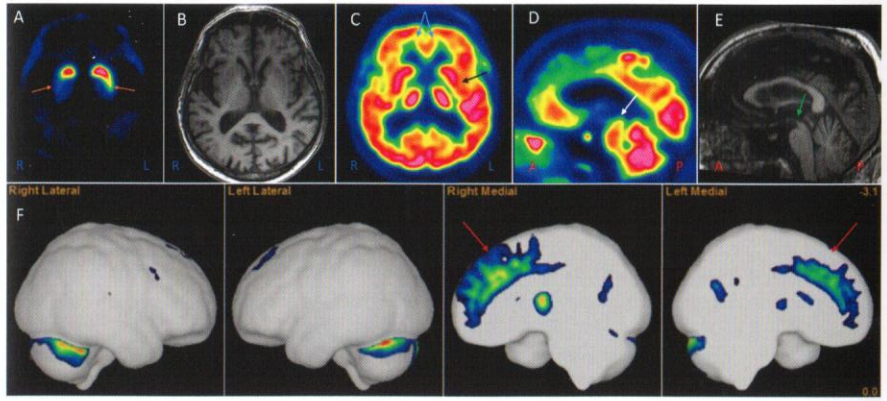

Figure 4. Example of [11C]PE2I PET/MR images in a patient with progressive supranuclear palsy with predominantly left-sided clinical symptoms, axial rigidity and impaired eye gaze. (A) [11C]PE2I images of DAT availability showing reduced uptake in striatum (orange arrows), more pronounced on the right side. (B) MR image (T1-weighted sequence) showing no abnormalities in the striatum. (C) [11C]PE2I image of rCBF showing decreased perfusion bilaterally in medial frontal cortex (blue arrows) and in left putamen (black arrow). (D) [11C]PE2I image of rCBF showing decreased perfusion in midbrain (white arrow). (E) MR image (T1-weighted sequence) showing midbrain atrophy (green arrow). (F) 3D surface projection map showing perfusion z-scores compared to a healthy control database, indicating decreased perfusion bilaterally in medial frontal cortex and anterior cingulate gyrus (red arrows).

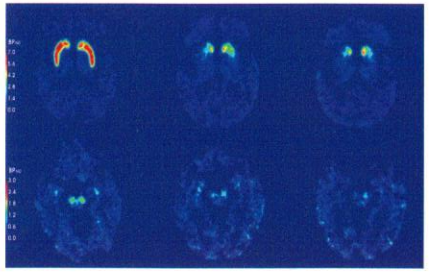

Figure 5. Representative images of [18F]FE-PE2I BP_{ND} in the striatum (upper section) and substantia nigra (lower section) of 67-year-old healthy male control (on the left) and a 68-year-old male patient with Parkinson's disease, with a UPDRS motor score of 23 and a disease duration of 2 years at the baseline (in the centre) and after a 2-year follow-up (on the right).

RADIATION EXPOSURE

[11C]PE2I

The effective dose from [11C]PE2I is 0.0064 mSv/MBq, and the organs receiving the highest equivalent doses are the urinary bladder wall, kidneys, and stomach (19). The tracer is mainly eliminated through renal clearance (Table 4). Typical administered activity is 350 MBq per 70 kg body weight.

[18F]FE-PE2I

The effective dose from [18F]FE-PE2I is 0.023 mSv/MBq, and the organs receiving the highest equivalent doses are the urinary bladder wall, liver, and pancreas (21). These values are comparable with other 18F-labelled radioligands for brain imaging. The tracer is eliminated via both gastrointestinal and renal clearance (Table 4). Typical administered activity is 185–200 MBq per 70 kg body weight.

Radiotracer	Organs receiving the highest absorbed dose	mGy/MBq	Effective dose per injected activity
[11C]PE2I	Urinary bladder wall	0.018	0.0064
	Kidneys	0.016	
	Stomach	0.014	
[18F]FE-PE2I	Urinary bladder wall	0.119	0.023
	Liver	0.046	
	Pancreas	0.031	

Table 4. Critical organs, equivalent and effective dose for [11C]PE2I and [18F]FE-PE2I.

REFERENCES

1. Giros B, Caron MG. Molecular characterization of the dopamine transporter. Trends Pharmacol Sci. 1993;14(2):43-9.
2. Nirenberg MJ, Vaughan RA, Uhl GR, Kuhar MJ, Pickel VM. The dopamine transporter is localized to dendritic and axonal plasma membranes of nigrostriatal dopaminergic neurons. J Neurosci. 1996;16(2):436-47.
3. Hersch SM, Yi H, Heilman CJ, Edwards RH, Levey AI. Subcellular localization and molecular topology of the dopamine transporter in the striatum and substantia nigra. J Comp Neurol. 1997;388(2):211-27.
4. DATSCAN (ioflupane I 123 injection), for intravenous use [cited 2024 JAN 19]. Available from: https://www.accessdata.fda.gov/drugsatfda_docs/label/2022/022454s010lbl.pdf.
5. DaTSCAN, Ioflupane (I-123) [cited 2024 JAN 19]. Available from: https://www.ema.europa.eu/en/documents/product-information/datscan-epar-product-information_en.pdf.
6. Varrone A, Halldin C. Molecular imaging of the dopamine transporter. J Nucl Med. 2010;51(9):1331-4.
7. Varrone A, Halldin C. New developments of dopaminergic imaging in Parkinson's disease. Q J Nucl Med Mol Imaging. 2012;56(1):68-82.
8. Muller L, Halldin C, Farde L, Karlsson P, Hall H, Swahn CG, et al. [11C] beta-CIT, a cocaine analogue. Preparation, autoradiography and preliminary PET investigations. Nucl Med Biol. 1993;20(3):249-55.
9. Emond P, Garreau L, Chalon S, Boazi M, Caillet M, Bricard J, et al. Synthesis and ligand binding of nortropane derivatives: N-substituted 2beta-carbomethoxy-3beta-(4'-iodophenyl)nortropane and N-(3-iodoprop-(2E)-enyl)-2beta-carbomethoxy-3beta-(3',4'-disubstituted phenyl)nortropane. New high-affinity and selective compounds for the dopamine transporter. J Med Chem. 1997;40(9):1366-72.
10. Stepanov V, Schou M, Jarv J, Halldin C. Synthesis of 3H-labeled N-(3-iodoprop-2E-enyl)-2beta-carbomethoxy-3beta-(4-methylphenyl) nortropane (PE2I) and its interaction with mice striatal membrane fragments. Appl Radiat Isot. 2007;65(3):293-300.
11. Dolle F, Bottlaender M, Demphel S, Emond E, Fuseau C, Coulon C, et al. Highly efficient synthesis of [11C] PE2I, a selective radioligand for the quantification of the dopamine transporter using PET. J Labelled Cpd Radiopharm. 2000;43:997-1004.
12. Halldin C, Erixon-Lindroth N, Pauli S, Chou YH, Okubo Y, Karlsson P, et al. [(11)C]PE2I: a highly selective radioligand for PET examination of the dopamine transporter in monkey and human brain. Eur J Nucl Med Mol Imaging. 2003;30(9):1220-30.
13. Bratteby K, Denholt CL, Lehel S, Petersen IN, Madsen J, Erlandsson M, et al. Fully Automated GMP-Compliant Synthesis of [(18)F]FE-PE2I. Pharmaceuticals (Basel). 2021;14(7).
14. Schou M, Steiger C, Varrone A, Guilloteau D, Halldin C. Synthesis, radiolabeling and preliminary in vivo evaluation of [18F]FE-PE2I, a new probe for the dopamine transporter. Bioorg Med Chem Lett. 2009;19(16):4843-5.
15. Varrone A, Toth M, Steiger C, Takano A, Guilloteau D, Ichise M, et al. Kinetic analysis and quantification of the dopamine transporter in the nonhuman primate brain with 11C-PE2I and 18F-FE-PE2I. J Nucl Med. 2011;52(1):132-9.
16. Stepanov V, Krasikova RN, Raus L, Loog O, Hiltunen J, Halldin C. An efficient one-step radiosynthesis of [18F]FE-PE2I, a PET radioligand for imaging of dopamine transporters. Journal of Labelled Compounds and Radiopharmaceuticals. 2012;55:206-10.
17. Elsinga P, Todde S, Penuelas I, Meyer G, Farstad B, Faivre-Chauvet A, et al. Guidance on current good radiopharmacy practice (cGRPP) for the small-scale preparation of radiopharmaceuticals. European journal of nuclear medicine and molecular imaging. 2010;37:1049-62.
18. EDQM. Raclopride ([11C]Methoxy) injection European Pharmacopoeia 11.4 ed. Strasbourg, France: European Directorate for the Quality of Medicines & HealthCare; 2023.
19. EDQM. [18F]Fludeoxyglucose injection. European Pharmacopoeia 11.4 ed. Strasbourg, France: European Directorate for the Quality of Medicines & HealthCare; 2024.

20. Ory D, Van den Brande J, de Groot T, Serdons K, Bex M, Declercq L, et al. Retention of [(18)F]fluoride on reversed phase HPLC columns. J Pharm Biomed Anal. 2015;111:209-14.
21. Hirvonen J, Johansson J, Teras M, Oikonen V, Lumme V, Virsu P, et al. Measurement of striatal and extrastriatal dopamine transporter binding with high-resolution PET and [11C]PE2I: quantitative modeling and test-retest reproducibility. J Cereb Blood Flow Metab. 2008;28(5):1059-69.
22. Ribeiro MJ, Ricard M, Lievre MA, Bourgeois S, Emond P, Gervais P, et al. Whole-body distribution and radiation dosimetry of the dopamine transporter radioligand [(11)C]PE2I in healthy volunteers. Nucl Med Biol. 2007;34(4):465-70.
23. Seki C, Ito H, Ichimiya T, Arakawa R, Ikoma Y, Shidahara M, et al. Quantitative analysis of dopamine transporters in human brain using [11C] PE2I and positron emission tomography: evaluation of reference tissue models. Ann Nucl Med. 2010;24(4):249-60.
24. Lizana H, Johansson L, Axelsson J, Larsson A, Ogren M, Linder J, et al. Whole-Body Biodistribution and Dosimetry of the Dopamine Transporter Radioligand (18)F-FE-PE2I in Human Subjects. J Nucl Med. 2018;59(8):1275-80.
25. Fazio P, Svenningsson P, Forsberg A, Jonsson EG, Amini N, Nakao R, et al. Quantitative Analysis of (1)(8)F-(E)-N-(3-Iodoprop-2-Enyl)-2beta-Carbofluoroethoxy-3beta-(4'-Methyl-Phenyl) Nortropane Binding to the Dopamine Transporter in Parkinson Disease. J Nucl Med. 2015;56(5):714-20.
26. Fazio P, Svenningsson P, Cselenyi Z, Halldin C, Farde L, Varrone A. Nigrostriatal dopamine transporter availability in early Parkinson's disease. Mov Disord. 2018;33(4):592-9.
27. Morbelli S, Esposito G, Arbizu J, Barthel H, Boellaard R, Bohnen NI, et al. EANM practice guideline/SNMMI procedure standard for dopaminergic imaging in Parkinsonian syndromes 1.0. Eur J Nucl Med Mol Imaging. 2020;47(8):1885-912.
28. Appel L, Jonasson M, Danfors T, Nyholm D, Askmark H, Lubberink M, et al. Use of 11C-PE2I PET in differential diagnosis of parkinsonian disorders. J Nucl Med. 2015;56(2):234-42.
29. Jonasson M, Appel L, Engman J, Frick A, Nyholm D, Askmark H, et al. Validation of parametric methods for [11C] PE2I positron emission tomography. Neuroimage. 2013;74:172-8.
30. Sonni I, Fazio P, Schain M, Halldin C, Svenningsson P, Farde L, et al. Optimal Acquisition Time Window and Simplified Quantification of Dopamine Transporter Availability Using 18F-FE-PE2I in Healthy Controls and Parkinson Disease Patients. J Nucl Med. 2016;57(10):1529-34.
31. Brumberg J, Kerstens V, Cselenyi Z, Svenningsson P, Sundgren M, Fazio P, et al. Simplified quantification of [(18)F]FE-PE2I PET in Parkinson's disease: Discriminative power, test-retest reliability and longitudinal validity during early peak and late pseudo-equilibrium. J Cereb Blood Flow Metab. 2021;41(6):1291-300.
32. Jonasson M, Appel L, Danfors T, Nyholm D, Askmark H, Frick A, et al. Development of a clinically feasible [(11)C]PE2I PET method for differential diagnosis of parkinsonism using reduced scan duration and automated reference region extraction. Am J Nucl Med Mol Imaging. 2017;7(6):263-74.
33. Guedj E, Varrone A, Boellaard R, Albert NL, Barthel H, van Berckel B, et al. EANM procedure guidelines for brain PET imaging using [(18)F]FDG, version 3. Eur J Nucl Med Mol Imaging. 2022;49(2):632-51.
34. Jonasson M, Appel L, Roslin S, Antoni G, Nyholm D, Danfors T, et al. Within-subject comparison of 11C-PE2I and 18F-FE-PE2I PET for dopamine transporter availability and relative blood flow measures. EANM'23 Abstract Book Congress Sep 9-13, 2023. European Journal of Nuclear Medicine and Molecular Imaging. 2023;50(1):1-898.
35. Minoshima S, Frey KA, Koeppe RA, Foster NL, Kuhl DE. A diagnostic approach in Alzheimer's disease using three-dimensional stereotactic surface projections of fluorine-18-FDG PET. Journal of Nuclear Medicine. 1995;36(7):1238-48.
36. Ishii K, Kono AK, Sasaki H, Miyamoto N, Fukuda T, Sakamoto S, et al. Fully automatic diagnostic system for early-and late-onset mild Alzheimer's disease using FDG PET and 3D-SSP. European journal of nuclear medicine and molecular imaging. 2006;33:575-83.

37. Varrone A, Dickson JC, Tossici-Bolt L, Sera T, Asenbaum S, Booij J, et al. European multicentre database of healthy controls for [123I]FP-CIT SPECT (ENC-DAT): age-related effects, gender differences and evaluation of different methods of analysis. Eur J Nucl Med Mol Imaging. 2013;40(2):213-27.
38. Marek K, Jennings D, Lasch S, Siderowf A, Tanner C, Simuni T, et al. The Parkinson progression marker initiative (PPMI). Progress in neurobiology. 2011;95(4):629-35.
39. Kerstens VS, Fazio P, Sundgren M, Brumberg J, Halldin C, Svenningsson P, et al. Longitudinal DAT changes measured with [(18)F]FE-PE2I PET in patients with Parkinson's disease; a validation study. Neuroimage Clin. 2023;37:103347.

20. Ory D, Van den Brande J, de Groot T, Serdons K, Bex M, Declercq L, et al. Retention of [(18)F]fluoride on reversed phase HPLC columns. J Pharm Biomed Anal. 2015;111:209-14.
21. Hirvonen J, Johansson J, Teras M, Oikonen V, Lumme V, Virsu P, et al. Measurement of striatal and extrastriatal dopamine transporter binding with high-resolution PET and [11C]PE2I: quantitative modeling and test-retest reproducibility. J Cereb Blood Flow Metab. 2008;28(5):1059-69.
22. Ribeiro MJ, Ricard M, Lievre MA, Bourgeois S, Emond P, Gervais P, et al. Whole-body distribution and radiation dosimetry of the dopamine transporter radioligand [(11)C]PE2I in healthy volunteers. Nucl Med Biol. 2007;34(4):465-70.
23. Seki C, Ito H, Ichimiya T, Arakawa R, Ikoma Y, Shidahara M, et al. Quantitative analysis of dopamine transporters in human brain using [11C] PE2I and positron emission tomography: evaluation of reference tissue models. Ann Nucl Med. 2010;24(4):249-60.
24. Lizana H, Johansson L, Axelsson J, Larsson A, Ogren M, Linder J, et al. Whole-Body Biodistribution and Dosimetry of the Dopamine Transporter Radioligand (18)F-FE-PE2I in Human Subjects. J Nucl Med. 2018;59(8):1275-80.
25. Fazio P, Svenningsson P, Forsberg A, Jonsson EG, Amini N, Nakao R, et al. Quantitative Analysis of (1)(8)F-(E)-N-(3-Iodoprop-2-Enyl)-2beta-Carbofluoroethoxy-3beta-(4'-Methyl-Phenyl) Nortropane Binding to the Dopamine Transporter in Parkinson Disease. J Nucl Med. 2015;56(5):714-20.
26. Fazio P, Svenningsson P, Cselenyi Z, Halldin C, Farde L, Varrone A. Nigrostriatal dopamine transporter availability in early Parkinson's disease. Mov Disord. 2018;33(4):592-9.
27. Morbelli S, Esposito G, Arbizu J, Barthel H, Boellaard R, Bohnen NI, et al. EANM practice guideline/SNMMI procedure standard for dopaminergic imaging in Parkinsonian syndromes 1.0. Eur J Nucl Med Mol Imaging. 2020;47(8):1885-912.
28. Appel L, Jonasson M, Danfors T, Nyholm D, Askmark H, Lubberink M, et al. Use of 11C-PE2I PET in differential diagnosis of parkinsonian disorders. J Nucl Med. 2015;56(2):234-42.
29. Jonasson M, Appel L, Engman J, Frick A, Nyholm D, Askmark H, et al. Validation of parametric methods for [11C] PE2I positron emission tomography. Neuroimage. 2013;74:172-8.
30. Sonni I, Fazio P, Schain M, Halldin C, Svenningsson P, Farde L, et al. Optimal Acquisition Time Window and Simplified Quantification of Dopamine Transporter Availability Using 18F-FE-PE2I in Healthy Controls and Parkinson Disease Patients. J Nucl Med. 2016;57(10):1529-34.
31. Brumberg J, Kerstens V, Cselenyi Z, Svenningsson P, Sundgren M, Fazio P, et al. Simplified quantification of [(18)F]FE-PE2I PET in Parkinson's disease: Discriminative power, test-retest reliability and longitudinal validity during early peak and late pseudo-equilibrium. J Cereb Blood Flow Metab. 2021;41(6):1291-300.
32. Jonasson M, Appel L, Danfors T, Nyholm D, Askmark H, Frick A, et al. Development of a clinically feasible [(11)C]PE2I PET method for differential diagnosis of parkinsonism using reduced scan duration and automated reference region extraction. Am J Nucl Med Mol Imaging. 2017;7(6):263-74.
33. Guedj E, Varrone A, Boellaard R, Albert NL, Barthel H, van Berckel B, et al. EANM procedure guidelines for brain PET imaging using [(18)F]FDG, version 3. Eur J Nucl Med Mol Imaging. 2022;49(2):632-51.
34. Jonasson M, Appel L, Roslin S, Antoni G, Nyholm D, Danfors T, et al. Within-subject comparison of 11C-PE2I and 18F-FE-PE2I PET for dopamine transporter availability and relative blood flow measures. EANM'23 Abstract Book Congress Sep 9-13, 2023. European Journal of Nuclear Medicine and Molecular Imaging. 2023;50(1):1-898.
35. Minoshima S, Frey KA, Koeppe RA, Foster NL, Kuhl DE. A diagnostic approach in Alzheimer's disease using three-dimensional stereotactic surface projections of fluorine-18-FDG PET. Journal of Nuclear Medicine. 1995;36(7):1238-48.
36. Ishii K, Kono AK, Sasaki H, Miyamoto N, Fukuda T, Sakamoto S, et al. Fully automatic diagnostic system for early-and late-onset mild Alzheimer's disease using FDG PET and 3D-SSP. European journal of nuclear medicine and molecular imaging. 2006;33:575-83.

37. Varrone A, Dickson JC, Tossici-Bolt L, Sera T, Asenbaum S, Booij J, et al. European multicentre database of healthy controls for [123I]FP-CIT SPECT (ENC-DAT): age-related effects, gender differences and evaluation of different methods of analysis. Eur J Nucl Med Mol Imaging. 2013;40(2):213-27.
38. Marek K, Jennings D, Lasch S, Siderowf A, Tanner C, Simuni T, et al. The Parkinson progression marker initiative (PPMI). Progress in neurobiology. 2011;95(4):629-35.
39. Kerstens VS, Fazio P, Sundgren M, Brumberg J, Halldin C, Svenningsson P, et al. Longitudinal DAT changes measured with [(18)F]FE-PE2I PET in patients with Parkinson's disease; a validation study. Neuroimage Clin. 2023;37:103347.